Biogeosciences Discuss., 6, 8851–8881, 2009
www.biogeosciences-discuss.net/6/8851/2009/

Biogeosciences Discussions

Biogeosciences Discussions is the access reviewed discussion forum of *Biogeosciences*

Estimating mixed layer nitrate in the North Atlantic Ocean

T. Steinhoff[1], T. Friedrich[3], S. E. Hartman[2], A. Oschlies[1], D. W. R. Wallace[1], and A. Körtzinger[1]

[1]Leibniz Institut für Meereswissenschaften (IFM-GEOMAR), Kiel, Germany
[2]National Oceanography Centre, Southampton, UK
[3]International Pacific Research Center, School of Ocean and Earth Science and Technology, University of Hawaii at Manoa, Honolulu, Hawaii, USA

Received: 29 July 2009 – Accepted: 18 August 2009 – Published: 3 September 2009

Correspondence to: T. Steinhoff (tsteinhoff@ifm-geomar.de)

Published by Copernicus Publications on behalf of the European Geosciences Union.

Abstract

Here we present an equation for the estimation of nitrate in surface waters of the North Atlantic Ocean (40° N to 52° N, 10° W to 60° W). The equation was derived by multiple linear regression (MLR) from nitrate, sea surface temperature (SST) observational data and model mixed layer depth (MLD) data. The observational data were taken from merchant vessels that have crossed the North Atlantic on a regular basis in 2002/2003 and from 2005 to present. It is important to find a robust and realistic esitmate of MLD because the deepening of the mixed layer is crucial for nitrate supply to the surface. We compared model data from two models (FOAM and Mercator) with MLD derived from float data (using various criteria). The Mercator model gives a MLD estimate that is close to the MLD derived from floats. MLR was established using SST, MLD from Mercator, time and latitude as predictors. Additionally a neural network was trained with the same dataset and the results were validated against both model data as a "ground truth" and an independent observational dataset. This validation produced RMS errors of the same order for MLR and the neural network approach. We conclude that it is possible to estimate nitrate concentrations with an uncertainty of $\pm 1.5\,\mu\text{mol}\,\text{L}^{-1}$ in the North Atlantic.

1 Introduction

Estimating nutrient fluxes into the upper ocean and their subsequent utilisation by marine primary production is still a big challenge in oceanography. Even though there are continuous sampling programs at Bermuda Atlantic Time Series (BATS, Bates, 2007) station in the western North Atlantic and European Station for Time Series in the Ocean, Canary Islands (ESTOC, González-Dávila et al., 2007) in the eastern part of the subtropical North Atlantic, it is impossible to map nutrient variability for the whole basin. The mechanism of nutrient supply is very different at the two stations: at BATS it is mainly driven by eddies and at ESTOC by winter convection (Cianca et al., 2007).

Furthermore these two stations are located in the subtropical gyre where seasonality is low. In the temperate North Atlantic, between 30° N and 60° N, the coverage of surface nutrient data is sparse and far from seasonal coverage as wintertime observations are sparse. Körtzinger et al. (2008) and Hartman et al. (2009) report a seasonal cycle of nutrient data for the years 2003/2004 with data from a single location, Porcupine Abyssal Plain site (PAP), located in the temperate North East Atlantic Ocean (49° N,16.5° W).

Some work has been done to estimate winter nitrate concentrations from nitrate-density relationships (Garside and Garside, 1995), nitrate-temperature/density relationships (Kamykowski and Zentara, 1986; Sherlock et al., 2007) or to estimate nutrient fields from remotely sensed data (Goes et al., 2000; Kamykowski et al., 2002; Switzer et al., 2003). Several other attempts were made to estimate wintertime nitrate concentration (e.g. Takahashi et al., 1985; Glover and Brewer, 1988; Körtzinger et al., 2001; Koeve, 2001) as the preformed values at the onset of the productive season are crucial to assess new production (Minas and Codespoti, 1993).

Another useful application of predicting seasonal nutrient cycles, that are not based on climatology, is the parameterization of CO_2 partial pressure in seawater (pCO_2). Studies have been performed to relate the pCO_2 in the North Atlantic to remotely sensed data (Lefèvre et al., 2005; Jamet et al., 2007; Lüger et al., 2008; Chierici et al., 2009; Friedrich and Oschlies, 2009a,b; Telszewski et al., 2009) as it is driven by many factors: thermodynamics, biology, mixing and air-sea gas exchange. Chlorophyll a (chl-a) concentrations are often employed to estimate the biological driver of the pCO_2, but the utility of chl-a for this purpose is rather limited (Ono et al., 2004; Lüger et al., 2008). This is especially true if chl-a is derived from satellites as they only "see" the upper few meters of the surface ocean. Given that nitrate changes are directly related to new production we believe that estimation of the entire seasonal cycle of nitrate could also improve pCO_2 predictions.

Here we present (and compare) two methods using observational data to estimate mixed-layer nitrate in the North Atlantic between 40° N and 52° N and 10° W and 60° W.

The first method is a multi linear regression (MLR) and the second method used the same data to train a neural network.

However, the quality of any prediction depends on the quality of the predictors. Therefore we chose the variables to be used in the prediction, sea surface temperature (SST) and MLD, very carefully. Reliable and well tested SST products are available e.g. the Advanced Microwave Scanning Radiometer-EOS (AMSR-E) on NASA EOS Aqua satellite (Emery et al., 2006). The situation is more complicated for MLD because there is no uniform criterion for its estimation. Numerous criteria for the estimation of MLD can be found in the literature (e.g. Kara et al., 2003; de Boyer Montégut et al., 2004) and often the criteria need to be adjusted regionally. The proposed criteria vary from simple temperature difference criteria to advanced methods such as the curvature criterion of Lorbacher et al. (2006) that uses the shape of vertical profiles (temperature or density). For all these criteria temperature/density profiles are required for the MLD estimation. Alternatively, MLD climatologies or MLD estimates from models can be used. In this study we compare MLD calculated from in-situ measured profiles (i.e. by ARGO floats), MLD climatology of Monterey and Levitus (1997), and MLD estimates from two different models (FOAM and Mercator).

2 Data and calculations

2.1 Discrete water samples

We use data from water samples taken on "Volunteer Observing Ships" (VOS) along a trans-Atlantic route between Europe and North America (Fig. 1). These studies were part of two European research projects CArbon VAriability Studies by Ships Of Opportunity (CAVASSOO) and CARBOOCEAN. During CAVASSOO (2002/2003) samples were collected from the merchant vessel M/V Falstaff (Wallenius Lines, Stockholm, Sweden). The M/V Falstaff was used at the onset of CARBOOCEAN but was changed to a new ship, the M/V Atlantic Companion (Atlantic Container Lines, New Jersey, USA), in 2006. Both ships were outfitted with autonomous instruments that measure pCO_2 (Lüger et al., 2004). At the same time sea surface temperature (SST) and salinity (SSS) were measured using Seabird thermosalinographs (SBE21 or SBE45) with external SBE38 temperature sensors that were located near the seawater intake.

On both ships we employed the same sampling procedure for the nitrate samples: seawater was drawn into 60 mL plastic bottles that were immediately frozen at –18°C. They were kept frozen until measurement in the shore-based laboratory at the IFM-GEOMAR, Kiel, following the method of Hansen and Koroleff (1999). The overall accuracy of these samples is ±3% in the range of 0–10 μmol L^{-1}. In this study we use over 400 nitrate measurements that were taken at approximately 7 m depth from surface waters in the open ocean. Only samples taken at water depths deeper than 1000 m were used, in order to exclude any influence by shelf waters and the waters of the Labrador Current. The earlier data taken on the M/V Falstaff are located closer to the southern end of the study region, covering a latitudinal band between 40° N and 50° N. The data from the M/V Atlantic Companion are located closer to the north between 45° N and 55° N.

2.2 Mixed layer depth

We compared MLD estimations from the climatology of Monterey and Levitus (1997), the output of two ocean models, and calculated by applying different criteria on vertical temperature profiles measured by the ARGO float network in order to identify the most suitable MLD estimate. The data from the ARGO floats were collected and made freely available by the Coriolis project and programmes that contribute to it (http://www.coriolis.eu.org).

2.2.1 MLD calculated from ARGO data

We downloaded all profile data available for the time period 2002–2007 in our study region from the ARGO website. All profiles were linearly interpolated onto 5 m depth intervals. MLD was calculated only from temperature profiles for this comparison, because the number of profiles including both temperature and salinity is less than the number of temperature profiles. We note that calculations based on a temperature criterion represent the iso-thermal layer (ILD) which can be different from the MLD (Kara et al., 2003), but we assume this difference to be negligible for our comparison study. Thomson and Fine (2002) have shown that using temperature related MLD estimates are preferable for biological applications. We used only profiles with at least 10 data points, with the uppermost datapoints shallower than 15 m. For the specified time period we found more than 23 000 profiles. The MLD was calculated using the commonly used threshold difference method with various ΔT (ΔT=0.2°C, 0.5°C and 1°C). We used the uppermost data point of each profile (≤15 m) as the surface reference temperature. In addition to these simple difference criteria, we also applied the curvature criterion of Lorbacher et al. (2006) that defines the MLD by the curvature of the given profile (temperature or density). We used a Matlab® routine that was provided by the authors for the calculation.

2.2.2 Climatological MLD

The MLD climatology of Monterey and Levitus (1997) contains monthly MLD fields on a 1°×1° grid for the global ocean. MLD is calculated based on three different criteria: a temperature difference, a density difference, and a variable density change. As previous stated, we used only the data calculated with the temperature difference criterion, which employs a surface-to-depth difference of 0.5°C.

2.2.3 Modelled MLD

For the modelled MLD we chose the output from two models: (a) Forecasting Ocean Assimilation Model (FOAM) from the Met Office, UK, (http://www.ncof.co.uk/FOAM-System-Description.html) and (b) Mercator Project, France (http://www.mercator-ocean.fr). The two models provide daily MLD from 2002 with a spatial resolution of 1/8°×1/8° and 1/6°×1/6°, for FOAM and Mercator respectively. A difference criterion of 1°C for temperature and 0.05 kg m^{-3} for density is used in the FOAM model while difference criteria of 0.2°C and 0.01 kg m^{-3} are used for Mercator.

2.2.4 Comparison of MLD estimates

We randomly chose 31 temperature profiles from ARGO floats for the comparison, for which we calculated the MLD using the different criteria mentioned above. Figure 2 shows two typical examples of temperature profiles with the various MLD estimates. We also tried to manually identify a best MLD estimate as a reference point by the "eyeball" method, i.e. a phenomenological identification of the MLD. We determined the climatological value and the model data for this specific time and position and calculated the difference between the various MLD estimates and the "eyeball" reference MLD. The mean values for these 31 profiles are shown in Fig. 3. Although the criterion of Lorbacher et al. (2006) appears to yield the best MLD estimate, we decided to use the MLD output from the Mercator model (which is only slightly inferior) for further calculations for the following reasons: 1) Despite the huge number of floats in the ocean (3190 floats in 10/2008) the coverage is spatially and temporally sparse compared to the model, 2) existance of a diel cycle in the MLD (Price et al., 1986) may bias MLD estimation when using real profiles.

2.3 Multiple Linear Regression (MLR)

Our ultimate goal was to develop a predictive equation for mixed layer nitrate on the basis of variables that are publicly available. Our initial list of predictors were the following parameters: sea surface temperature (SST), MLD, latitude (Lat), longitude (Lon) and time (t), where t is the day of the year. To take into account that the first and the last day of a year have nearly the same influence on our dataset we performed a sinusoidal transformation to the actual day of the year analogous to Nojiri et al. (1999). We employed a common logarithmic expression of SST-nitrate relationship because SST shows rather large variability when the nitrate concentration is low (i.e. during summer time). The logarithmic formulation decreases this non-linear character of the SST. We explicitly used in situ SST and not remotely sensed data to keep the errors associated with the establishment of the algorithm as small as possible. The use of different SST products derived for example from satellites is discussed below. All MLRs were calculated using the STATISTICA® software package (StatSoft, Tulsa, USA). We opted for the stepwise method, where an additional predictive variable is added only when the estimates are statistically significantly improved by adding this variable. This ensures that the resulting equation includes only those available parameters that are necessary to estimate the nitrate cycle. Our set of predictive variables results in the following best-fit equation:

$$NO_3 = 0.274 \times \mathrm{Lat} - 5.445 \times \log(\mathrm{SST}) + 0.006 \times \mathrm{MLD} + 3.142 \times \sin(2\pi \frac{t}{365}) + 1.110 \times \cos(2\pi \frac{t}{365}) - 3.345 \quad (1)$$

where nitrate is in μmol L^{-1}, SST in °C, MLD in m and t denotes the day of the year. 413 datapoints were used for the MLR and the adjusted R^2 value is 0.82. Note that longitudinal information turned out to be insignificant.

2.4 Self-Organizing Map (SOM)

The regression coefficients provide information about physical relationships between nitrate and SST or MLD, respectively, if the predictors of a MLR are independent. The drawback of this method is the limitation to a linear relation and (even for a polynomial regression) the fitting to a predefined function. Therefore, a neural network approach was additionally employed using a self-organizing map. SOMs were introduced to science by Kohonen (1982) and successfully applied to oceanographic data by Lefèvre et al. (2005), Friedrich and Oschlies (2009a,b) and Telszewski et al. (2009). SOMs are able to estimate a target value (e.g. nitrate) from related parameters (e.g. MLD, SST) without fitting to a predefined function by recognizing relationships in the observational data during the training process. The same predictive parameters used in the MLR (Eq. 1) were employed in the SOM.

2.5 Algorithm validation

2.5.1 Validation against observational data

We performed several tests to evaluate the predictive power of the algorithm for mixed layer nitrate (Eq. 1) and for the SOM estimations. The MLR (Fig. 4) shows that the calculated data are generally in good agreement with the measurements, although there are obvious differences in spring and autumn. Negative nitrate values are predicted during the summer when nitrate is depleted but for a simple linear approach allowing for random error the prediction of negative values is the only way to produce a period of zero nitrate. All predicted negative values were set to zero for further calculations. The higher deviations in spring and autumn may arise from small scale variability (patchiness) and cannot be reproduced through our simple MLR approach. The resulting RMS error of this first validation is 1.3 μmol L^{-1}. In addition, we randomly chose 100 data points to exclude from the entire dataset and performed a MLR with the remaining data. The coefficients of the resulting equation were of the same order as the ones in (Eq. 1). We used this equation to estimate the nitrate concentration for the 100 data points we deleted for the MLR. We performed this test three times and calculated the RMS error for the chosen data points each time. The resulting RMS errors were between 1.2 μmol L^{-1} and 1.6 μmol L^{-1}.

Another way to validate the predictive capacity of the algorithm is to plot predicted versus measured data (Fig. 5a). We performed an orthogonal regression for this data set because a linear regression is not appropriate for comparison in which both parameters are associated with random error for details refer to e.g. Castellaro et al. (2006). Both regression lines are shown. The orthogonal regression is slightly steeper with a slope of 0.87. We also show the 1:1 line for comparison. The MLR calculated nitrate is overestimated at low values and underestimated at high values, as expected (Fig. 5b).

We also employed a completely independent data set for comparison. During CAVASSOO the National Oceanography Center, Southampton, UK (NOC) took nitrate samples onboard the VOS M/V Santa Lucia and M/V Santa Maria, respectively. Both ships were sailing between the UK and Carribean (Fig. 1) and produced more than 600 nitrate samples between May 2002 and December 2003 in the area north of 40° N. We used the SST from their datset and the matching MLD from Mercator to estimate corresponding nitrate data with both methods: SOM and MLR. Since we do not have the MLD for all 2002 dates we included only 344 datapoints. The resulting RMS error is 1.5 μmol L^{-1} for the MLR as well as for the SOM estimates. Using only data between 10° W and 50° W (the SOM was trained only in this region) the RMS error is 1.3 μmol L^{-1} for the SOM method and 1.4 μmol L^{-1} for the MLR.

Figure 6 shows the intra and interannual variability of SST, MLD and nitrate concentration for the time period between 2002 and 2007 for two example locations: east (49° N, 16.5° W, PAP) and west (40° N, 49° W) of the North Atlantic. SST and nitrate measurements are also available for a whole annual cycle in 2002/2003 at the PAP site (Körtzinger et al., 2008), resulting in another independent dataset. The West Atlantic location was chosen in this region to illustrate the limitations of a MLR approach because the Labrador current may introduce short term variability on a daily timescale. The corresponding SST and nitrate values were added to the plot if one of the VOS line mentioned above crossed an area of 1°×1° (2°×2°) latitude/longitude around the location within one day. The annual amplitude of SST is more pronounced in the western region and the short term variability is also higher. The VOS SST measurements are in good agreement with AMSR-E in the eastern region. Deviations can be seen in the westerly region due to the high short term variability there, especially if data are from a 2°×2° grid cell. This short term variability at the westerly location also results in deviation of the VOS measured nitrate data from the predicted concentrations.

The instruments at PAP were deployed in approximately 30 m depth and Körtzinger et al. (2008) excluded data that were measured below the thermocline. The SST data measured at PAP and from the VOS lines agree with the data from AMSR-E. This results in good agreement between measurements and prediction of nitrate. In contrast to the measured nitrate data the (MLR) calculated nitrate data show a smooth seasonality. A comparison of the latter two results in a RMS error of 0.9 μmol L^{-1}. A comparison of the SOM calculated data and the measured values at PAP results in a RMS error of 1.4 μmol L^{-1}.

These tests illustrate that it is not possible to reproduce nitrate in the North Atlantic better than approximately ±1.5 μmol L^{-1} with the chosen parameter. The algorithm works well in predicting nitrate within the spatial and temporal domain of the data. The remaining uncertainty may arise from advective processes (Hartman et al., 2009), that are hard to assess by a linear interpolation, sampling errors arising from sample preservation and measurements, and variability in the causal links between the predictors and nitrate.

2.5.2 Validation using a biogeochemical model

Predicted nitrate concentrations were also validated against nitrate concentrations predicted by a high-resolution nitrogen-based nitrate-phytoplankton-zooplankton-detritus model of the North Atlantic. All model details are described in Oschlies et al. (2000) and Eden and Oschlies (2006). The advantage of this model-based validation is that the model produces daily nitrate fields with a horizontal resolution of $1/12^{\circ} \times 1/12^{\circ}$ cos(Lat) which can be used as a basinwide "ground-truth" to assess the accuracy of the nitrate estimates generated by the MLR and the SOM, respectively. The model output of SST, MLD and nitrate was sampled according to the time (day of the year) and position of the actual nitrate measurements during the period of June 2002 to May 2003, where error of nitrate measurements wasn't considered. This model-generated data set was then used to calculate a MLR and to train a SOM. The input parameters for both approaches were the same as for the observational data: Lat, SST, MLD, time (day of the year). Monthly mean model output of SST and MLD were used to generate nitrate estimates from both methods. Figure 7i shows the annual cycle of nitrate simulated by the model in the domain covered by the nitrate sampling (40° N to 52° N , 10° W to 50° W) and the annual cycle of the nitrate estimates derived from the model-generated data set by the MLR and the SOM, respectively. The general pattern of the annual cycle can be reproduced by the estimates. High winter nitrate concentrations are underestimated. The SOM estimate has a higher accuracy in reproducing the late summer nitrate minimum. It is apparent that the mapping fails in the north-western part of the basin because of the spatial and temporal distribution of the nitrate mapping error (Fig. 7a–d (MLR) and 7e-h (SOM)). This applies for both the MLR and for the SOM. High nitrate values occurring in the Labrador current cannot be reproduced by either estimate. This disparity may be due to the sparse observational coverage of the considered region or to the highly variable current system in this region. The basinwide RMS-error for our model-based validation amounts to 2.1 μmol L^{-1} for the SOM estimate and 2.2 μmol L^{-1} for the MLR estimate which is significantly higher than the error derived from the validation against independent observational data.

2.5.3 Error estimation when using remotely sensed data

Olsen et al. (2004) analysed the deviation between satellite derived SST and in situ measured SST. They found differences of up to 1°C. The minimum and maximum SST within our dataset is 5.9°C and 25.6°C, respectively. The maximum error would be between 4% and 20%. An error of 20% (4%) in SST would result in an error in nitrate of 0.4 μmol L^{-1} (0.1 μmol L^{-1}). In contrast, Emery et al. (2006) showed that the Advanced Microwave Scanning Radiometer-EOS (AMSR-E) on NASA EOS Aqua satellite produces SST data that are in good agreement with the in situ measured SST. We suggest that using the temperature from AMSR-E (www.http://www.ssmi.com/amsr) will introduce only a small error.

To assess the influence of over/underestimation of MLD, we calculated the error in nitrate that will arise from an uncertainty of 50 m in the MLD. The resulting error is on the order of 0.3 μmol L^{-1}.

3 Discussion

3.1 MLD estimations and variability

Our results indicate that it is possible to find a robust MLD estimate with a good temporal and spatial resolution. Although using in-situ profiles results in the best estimation of the MLD at a specific position and time the resolution of the ARGO network is too sparse for reflecting an annual cycle of MLD on the scale of the entire North Atlantic Ocean. In contrast, climatological MLD estimates (e.g. Monterey and Levitus, 1997; de Boyer Montégut et al., 2004) have uniform resolution but do not reflect interannual changes and show considerable deviations from observations (e.g. tend to significantly overpredict MLD). Using MLD generated by models could be a compromise: data are produced on a daily basis, on a regular grid, and can be in good agreement with observations. Here we compare results from two models since the model dependent differences are large.

For in-situ profiles, such as those measured by floats, the curvature criterion of Lorbacher et al. (2006) results in MLD that are closest to those which are eyeball-defined (Fig. 3). The model output from FOAM yields MLD that are significantly deeper than in-situ observations. This finding is in good agreement with de Boyer Montégut et al. (2004) who, among others, showed that a temperature criterion of 1°C (see Sect. 2.2.3) is too large for the subpolar North Atlantic. We choose the model output of the Mercator project, as this provides high resolution and MLD that are close to the eyeball-defined MLD.

We examined the variability in the reliably estimated MLD during the entire time period to understand the dynamics in the region. The mixed layer in the subpolar North Atlantic shows a clear seasonality (Fig. 6): during summer the MLD may be only a few tens of meters while, in wintertime, depths greater than 350 m can be reached. We carefully inspected the dynamics of the winter MLD since its deepening supplies nutrients to the sea surface (Oschlies, 2002). This makes the MLD one of the main forcing features in this regions biogeochemistry (Oschlies, 2002). It is well known that the

BGD
6, 8851–8881, 2009

maximum winter MLD increases with latitude and numerous studies have shown that a local maximum in the winter MLD exists between 45° N and 50° N in the North Atlantic (e.g. Koeve, 2001; de Coëtlogon and Frankignoul, 2003). The region of occurrence of the maximum MLD is known to be a region of most intense wintertime ocean heat loss (Marshall, 2005). Due to this rapid cooling at the surface the density rapidly increases and the surface waters along the North Atlantic Drift (NAD) are mixed much deeper than to the north and south of this region. Figure 8 shows the MLD as calculated by Mercator for 10 March 2006. The maximum MLD along the NAD is clearly visible.

3.2 Nitrate estimations

The nitrate data show a clear seasonality, with nitrate depleted during summer and the highest values in spring (8–12 μmol L^{-1}). The data during summer show low variability due to depletion of nitrate in the whole study area. Higher scatter can be observed in the data during the rest of the year. This is probably due to small scale variability of the sampled surface water (patchiness) as well as to the large latitudinal range of the cruise tracks (Fig. 1).

As expected, the latitudinal and time dependent terms in the MLD-algorithm explain most of the nitrate variability (Garcia et al., 2006). The latitudinal dependence was mentioned in various studies (e.g. Koeve, 2001; Kamykowski et al., 2002) and, together with the time dependent terms, represents a climatological annual nitrate cycle that is very stable within our study area. The small interannual variations (e.g. Fig. 6) can be explained by the fact that the data fall in nearly one biogeographic province as defined by Oliver and Irwin (2008). Following the classification of Longhurst (2007), our sampling area covers three provinces (gulf stream (GFST), North Atlantic drift (NADR) and North Atlantic subtropical gyre (NAST(E)) province). There are certain differences between these provinces, but the ecological processes are primarily driven by the same physical processes. Longhurst (2007) defined 6 cases of physical control, of which GFST and NADR are assigned to the same case: “nutrient-limited spring production peak”. NAST(E) is assigned to another case (“winter-spring production with nutrient limitation") but these samples contribute only 5% of our dataset and are located at the northern border of the NAST(E) province. As the borders between the certain provinces are not very strict, we can state that our dataset also fits in one biogeographical province as defined by Longhurst (2007).

The algorithm can be adjusted to capture the interannually varying conditions (providing they are not taken from climatologies) by adding SST and MLD. They reflect the actual conditions that can drive biological production and can change from year to year as well as from one place to another. The MLD appears to be a good indicator of the variable vertical supply of nitrate. The increase in winter time mixed layer between 2004 and 2007 (Fig. 6, middle panels) in both basins, east and west, results in an increase in nitrate concentrations. Figure 9a–c shows averaged values of the February/March data of MLD, SST and estimated MLR nitrate concentration at PAP site.

The overall uncertainty in predicting nitrate with the presented MLR-algorithm and SOM is 1.5 μmol L^{-1}. Initially this does not appear to be better than algorithms presented in former studies (e.g. Kamykowski and Zentara, 1986; Garside and Garside, 1995; Goes et al., 2000; Kamykowski et al., 2002; Switzer et al., 2003). Here we present one simple algorithm for a whole region that is easy to use and the desired input data (MLD, SST) can be accessed easily. In this study, the SOM predicted nitrate data are not better than the MLR estimates. We speculate that taking advantage of the benefits of SOM would require better data coverage.

We obtain an RMS error of 1.5 μmol L^{-1} when we use an independent dataset to calculate nitrate, which provides additional confidence in the algorithm. Furthermore this finding is consistent with those of Dore et al. (1996) since it shows again that keeping the nutrient samples frozen (at −18 to −20°C) until measurement is an acceptable way to preserve the dissolved inorganic nitrate (at least for open ocean waters).

The basinscale validation of the MLR and the SOM against a biogeochemical model produced RMS errors of 2.1 μmol L^{-1} (SOM) and 2.2 μmol L^{-1} (MLR) respectively. These errors are considerably larger than those obtained from the validation against independent observational data. In particular high nitrate values in winter and spring in the Labrador Current region could not have been reproduced by our estimation techniques. This clearly shows the temporal and spatial limitations of the presented method. The predictive potential of both techniques is mostly restricted to interpolation between lines of observations. An extrapolation to water masses not or barely covered by the variability range of the measurements suffers from larger estimation errors.

3.3 Implications of nitrate estimation to pCO_2

We calculated the increase in pCO_2 that should result from increased nitrate concentration as mentioned above (Fig. 9b): We assume that the nitrate concentration until 2005 constitutes a baseline and that the associated dissolved inorganic carbon (DIC) supply will result in pCO_2 values that are in equilibrium with the atmosphere. We find that the increased nitrate and the associated increased DIC (calculated from C/N ratio of 7.2 (Körtzinger et al., 2001)) will result in pCO_2 values that are increasing faster than the atmosphere (Fig. 9d). Both rates of pCO_2 increase are within the range of previous observations (Takahashi et al., 2009, and references herein) and we speculate that the observed changes in rates of pCO_2 increase may be due to the variable winter MLD and, thus, the nitrate supply.

As mentioned above a lot of effort is being made to predict seawater pCO_2 in the North Atlantic Ocean very precisely using remotely sensed data. One important driving force of the pCO_2 is the SST due to the thermodynamic effect, that is well known (e.g. Takahashi et al., 1993). But the pCO_2 is also affected by high biological activity (Watson et al., 1991; Lüger et al., 2004; Körtzinger et al., 2008) especially in the temperate North Atlantic which is hard to assess by remote sensing (Ono et al., 2004; Lüger et al., 2008, and references herein) as satellite chlorophyll data proved to be rather useless as a predictor in their study. As the biological production in the world oceans follows a nearly constant stoichiometry (Redfield et al., 1963) it is easy to calculate the change in DIC from a known nitrate change and subsequently the effect on pCO_2 can be calculated. Following the MLR approach of other studies but substituting satellite chlorophyll with calculated nitrate using the algorithm presented above has the potential to obtain better pCO_2 estimates. A residual error of 1.5 μmol L^{-1} in nitrate would still translate, however, into a pCO_2 error of $\geq$18 μatm. One could argue in favour of using the MLD and SST twice (first for the nitrate estimation and second for the pCO_2 estimation) as the SST dependence of pCO_2 is different from the dependence of nitrate.

This hypothesis has to be tested in future work and also the ongoing research onboard VOS lines will produce more nitrate data that could support and/or improve the presented algorithm and especially the SOM approach will become more important with a larger dataset.

Acknowledgements. We thank the captains and crews of M/V Falstaff, M/V Atlantic Companion, M/V Santa Maria and M/V Santa Lucia for their support. We would also like to thank all the people involved in taking/measuring the nitrate samples. Mooring data and support for this research was provided by the European research projects ANIMATE (Atlantic Network of Interdisciplinary Moorings and Time-Series for Europe), MERSEA (Marine Environment and Security for the European Sea) and EUR-OCEANS (European Network of Excellence for Ocean Ecosystems Analysis). This route of M/V Santa Maria and M/V Santa Lucia is used by the CAVASSOO (Carbon Variability Studies by Ships Of Opportunity) project to investigate seasonal and year-to-year variations in carbon fluxes in the North Atlantic. More information on CAVASSOO (EC funded between November 2000 and November 2003, EC grant number EVK2-CT-2000-00088) on: http://tracer.env.uea.ac.uk/e072/. This work was supported by the European Commission under the CARBOOCEAN project GOCE 511176-2.

References

Bates, N. R.: Interannual variability of the oceanic CO_2 sink in the subtropical gyre of the North Atlantic Ocean over the last 2 decades, J. Geophys. Res., 112, C09013, doi:10.1029/2006JC003759, 2007. 8852

Castellaro, S., Mulargia, F., and Kagan, Y.: Regression problems for magnitudes, Geophys. J. Int., 165, 913–930, doi:10.1111/j.1365-246X.2006.02955.x, 2006. 8859

Chierici, M., Olsen, A., Johannessen, T., Trinañes, J., and Wanninkhof, R.: Algorithms to estimate the carbon dioxide uptake in the northern North Atlantic using shipboard observations, satellite and ocean analysis data, Deep-Sea Res. II, 56, 630–639, 2009. 8853

Cianca, A., Helmke, P., Mouriño, B., Rueda, M. J., Llinás, O., and Neuer, S.: Decadal analysis of hydrography and in situ nutrient budgets in the western and eastern North Atlantic subtropical gyre, J. Geophys. Res., 112, C07025, doi:10.1029/2006JC003788, 2007. 8852

de Boyer Montégut, C., Madec, G., Fischer, A. S., Lazar, A., and Iudicone, D.: Mixed layer depth over the global ocean: An examination of profile data and profile-based climatology, J. Geophys. Res., 109, C12003, doi:10.1029/2004JC002378, 2004. 8854, 8863

de Coëtlogon, G. and Frankignoul, C.: The persistence of Winter Sea Surface Temperature in the North Atlantic, J. Climate, 16, 1364–1377, 2003. 8864

Dore, J. E., Houlihan, T., Hebel, D. V., Tien, G., Tupas, L., and Karl, D. M.: Freezing as a method of sample preservation for the analysis of dissolved inorganic nutrients in seawater, Mar. Chem., 53, 173–185, 1996. 8865

Eden, C. and Oschlies, A.: Adiabatic reduction of circulation-related CO_2 air-sea flux biases in a North Atlantic carbon-cycle model, Global Biogeochem. Cy., 20, GB2008, doi:10.1029/2005GB002521, 2006. 8861

Emery, W., Brandt, P., Funk, A., and Böning, C.: A comparison of sea surface temperatures from microwave remote sensing of the Labrador Sea with in situ measurements and model simulations, J. Geophys. Res., 111, C12013, doi:10.1029/2006JC003578, 2006. 8854, 8862

Friedrich, T. and Oschlies, A.: Neural network-based estimates of North Atlantic surface pCO_2 from satellite data: A methodological study, J. Geophys. Res., 114, C03020, doi:10.1029/2007JC004646, 2009a. 8853, 8858

Friedrich, T. and Oschlies, A.: Basin-scale pCO_2 maps estimated from ARGO float data – a model study, J. Geophys. Res., submitted, 2009b. 8853, 8858

Garcia, H., Locarnini, R., Boyer, T., and Antonov, J.: Volume 4: Nutrients (phosphate, nitrate, silicate), in: World Ocean Atlas 2005, edited by Ed. NOAA Atlas NESDIS 64, U. G. P. O., S. Levitus, 396 pp., 2006. 8864

Garside, C. and Garside, J. C.: Euphotic-zone nutrient algorithms for the NABE and EqPac study site, Deep-Sea Res.II, 42, 335–347, 1995. 8853, 8865

Glover, D. M. and Brewer, P. G.: Estimates of wintertime mixed layer nutrient concentration in the North Atlantic, Deep-Sea Res., 35, 1525–1546, 1988. 8853

Goes, J. I., Saino, T., Oaku, H., Ishizaka, J., Wong, C. S., and Nojiri, Y.: Basin scale estimates of sea surface nitrate and new production from remotely sensed sea surface temperature and chlorophyll, Geophys. Res. Lett., 27, 1263–1266, 2000. 8853, 8865

González-Dávila, M., Santana-Casiano, J. M., and González-Dávila, E. F.: Interannual variabil-

ity of the upper ocean carbon cycle in the northeast Atlantic Ocean, Geophys. Res. Lett., 34, L07608, doi:10.1029/2006GL028145, 2007. 8852
Hansen, H. and Koroleff, F.: Determination of nutrients, in: Methods of seawater analysis, edited by Grasshoff, K., Kremling, K., and Erhardt, M., Verlag Chemie, Weinheim, Germany, 159–228, 1999. 8855
Hartman, S. E., Larkin, K. E., Lampitt, R. S., Lankhorst, M., and Hydes, D. J.: Seasonal and inter-annual biogeochemical variations at PAP (49N, 16.5W) 2003–2005 associated with winter mixing and surface circulation, Deep Sea Res. II, submitted, 2009. 8853, 8861
Jamet, C., Moulin, C., and Lefévre, N.: Estimation of the oceanic pCO_2 in the North Atlantic from VOS lines in-situ measurements: parameters needed to generate seasonally mean maps, Ann. Geophys., 25, 2247–2257, 2007, http://www.ann-geophys.net/25/2247/2007/. 8853
Kamykowski, D. and Zentara, S. J.: Predicting plant nutrient concentration from temperature and sigma-*t* in the upper Kilometer of the world ocean, Deep-Sea Res. A, 33, 89–105, 1986. 8853, 8865
Kamykowski, D., Zentara, S. J., Morrison, J. M., and Switzer, A. C.: Dynamic global patterns of nitrate, phosphate, silicate, and iron, Global Biogeochem. Cy., 16(4), p. 1077, 2002. 8853, 8864, 8865
Kara, A. B., Rochford, P. A., and Hurlburt, H. E.: Mixed layer depth variability over the global ocean, J. Geophys. Res., 108(C3), 3079, doi:10.1029/2000JC000736, 2003. 8854, 8856
Koeve, W.: Wintertime nutrients in the Noth Atlantic – new approaches and implications for new production estimates, Mar. Chem., 74, 245–260, 2001. 8853, 8864
Kohonen, T.: Self-Organized Formation of Topologically Correct Feature Maps, Biol. Cybern., 43, 59–69, 1982. 8858
Körtzinger, A., Koeve, W., Kähler, P., and Mintrop, L.: C:N ratios in the mixed layer during the productive season in the northeast Atlantic Ocean, Deep-sea Res.I, 48, 661–688, 2001. 8853, 8866
Körtzinger, A., Send, U., Lampitt, R. S., Hartman, S., Wallace, D. W. R., Karstensen, J., Villagarcia, M. G., Llinás, O., and DeGrandpre, M. D.: The seasonal pCO_2 cycle at 49N/16.5W in the northeastern Atlantic Ocean and what it tells us about biological productivity, J. Geophys. Res., 113, C04020, doi10.1029/2007JC004347, 2008. 8853, 8860, 8866
Lefèvre, N., Watson, A. J., and Watson, A. R.: A comparison of multiple regression and neural network techniques for mapping *in situ* pCO_2 data, Tellus, 57B, 375–384, 2005. 8853, 8858

Longhurst, A. R.: Ecological geography of the sea, Academic Press, Boston, 2nd edn., 2007. 8864, 8865

Lorbacher, K., Dommenget, D., Niiler, P., and Köhl, A.: Ocean mixed layer depth: A subsurface proxy of ocean-atmosphere variability, J. Geophys. Res., 111, C07010, doi:10.1029/2003JC002157, 2006. 8854, 8856, 8857, 8863, 8875

Lüger, H., Wallace, D. W. R., Körtzinger, A., and Nojiri, Y.: The $p\mathrm{CO_2}$ varability in the mid-latitude North Atlantic Ocean during a full annual cycle, Global Biochem. Cy., 18, GB3023, doi:10.1029/2003GB002200, 2004. 8855, 8866

Lüger, H., Wanninkhof, R., Olsen, A., Trinañes, J., Johannessen, T., Wallace, D., and Körtzinger, A.: The sea-air CO_2 flux in the North Atlantic estimated from sattelite and ARGO profiling data, Tech. rep., NOAA, OAR AOML-96, 2008. 8853, 8866

Marshall, J.: CLIMODE: a mode water dynamics experiment in support of CLIVAR, Clivar Variations, 3(2), 8–14, 2005. 8864

Minas, H. J. and Codespoti, L. A.: Estimates of primary production by observation of changes in the mesoscale nitrate field, ICES Mar. Sci. Symp., 197, 215–235, 1993. 8853

Monterey, G. and Levitus, S.: Seasonal Variability of the Mixed Layer Depth for the World Ocean, in: NOAA Atlas NESDIS 14,96 pp., US Gov. Printing Office, Wash., D.C., 1997. 8854, 8855, 8856, 8863

Nojiri, Y., Fujinuma, Y., Zeng, J., and Wong, C.: Monitoring of $p\mathrm{CO_2}$ with complete seasonal coverage utilizing a cargo ship M/S Skaugran between Japan and Canada/US, in: Proceedings of the 2nd International Symposium CO_2 in the Oceans, CGER/NIES, 1999. 8857

Oliver, M. J. and Irwin, A. J.: Objective global ocean biogeographic provinces, Geoph. Res. Lett., 35, L15601, doi:10.1029/2008/GL034238, 2008. 8864

Olsen, A., Trinañes, J. A., and Wanninkhof, R.: Sea-air flux of CO_2 in the Caribbean Sea estimated using in situ and remote sensing data, Rem. Sens. Environ., 89, 309–325, 2004. 8862

Ono, T., Saino, T., Kurita, N., and Sasaki, K.: Basin-scale extrapolation of shipboard $p\mathrm{CO_2}$ data by using satellite SST and Chl*a*, Int. J. Rem. Sens., 25(19), 3803–3815, 2004. 8853, 8866

Oschlies, A.: Nutrient supply to the surface waters of the North Atlantic: A model study, J. Geophys. Res., 107, 3046, doi:10.1029/2000JC000275, 2002. 8863

Oschlies, A., Koeve, W., and Garçon, V.: An eddy-permitting coupled physical-biological model of the North Atlantic. Part 2: Ecosystem dynamics and comparison with satellite and JGOFS local studies data, Global Biogeochem. Cy., 14, 499–523, 2000. 8861

Price, J. F., Weller, R. A., and Pinkel, R.: Diurnal Cycling: Observations and Models of the Upper Ocean Response to, J. Geophys. Res., 91, 8411–8427, 1986. 8857

Redfield, A. C., Ketchum, B. H., and Richards, F. A.: The influence of organisms on the composition of seawater, in: The Sea, Vol.2, edited by Hill, M., 2, 26–77, Interscience, New York, 1963. 8866

Sherlock, V., Pickmere, S., Currie, K., Hadfield, M., Nodder, S., and Boyd, P. W.: Predictive accuracy of temperature-nitrate relationships for the oceanic mixed layer of the New Zealand region, J. Geophys. Res., 112, C06010, doi:10.1029/2006JC003562, 2007. 8853

Switzer, A. C., Kamykowski, D., and Zentara, S.-J.: Mapping nitrate in the global ocean using remotely sensed sea surface temperature, J. Geophys. Res., 108(C8), 3280, doi:10.1029/2000JC000444, 2003. 8853, 8865

Takahashi, T., Broeker, W. S., and Langer, S.: Redfield Ratio Based on Chemical Data from Isopycnal Surfaces, J. Geophys. Res., 90, 6907–6924, 1985. 8853

Takahashi, T., Olafsson, J., Goddard, J. G., Chipman, D. W., and Sutherland, S. C.: Seasonal Variation of CO_2 and Nutrients in the High-Latitude Surface Oceans: a comparative study, Global Biogeochem. Cy., 7, 843–878, 1993. 8866

Takahashi, T., Sutherland, S. C., Wanninkhof, R., Sweeney, C., Feely, R. A., Chipman, D. W., Hales, B., Friederich, G., Chavez, F., Sabine, C., Watson, A., Bakker, D. C., Schuster, U., Metzl, N., Yoshikawa-Inoue, H., Ishii, M., Midorikawa, T., Nojiri, Y., Körtzinger, A., Steinhoff, T., Hoppema, M., Olafsson, J., Arnarson, T. S., Tilbrook, B., Johannessen, T., Olsen, A., Bellerby, R., Wong, C., Delille, B., Bates, N., and de Baar, H. J.: Climatological mean and decadal change in surface ocean $p\mathrm{CO}_2$, and net sea-air CO_2 flux over the global oceans, Deep Sea Research Part II: Topical Studies in Oceanography, 56, 554–577, doi:10.1016/j.dsr2.2008.12.009, http://www.sciencedirect.com/science/article/B6VGC-4V59VVH-1/2/6c157bd4052048ac211736c038787a3a, surface Ocean CO_2 Variability and Vulnerabilities, 2009. 8866

Telszewski, M., Chazottes, A., Schuster, U., Watson, A. J., Moulin, C., Bakker, D. C. E., González-Dávila, M., Johannessen, T., Körtzinger, A., Lüger, H., Olsen, A., Omar, A., Pérez, F., Ríos, A., Steinhoff, T., Santana-Casiano, M., Wallace, D. W. R., and Wanninkhof, R.: Estimating the monthly $p\mathrm{CO}_2$ distribution in the North Atlantic using a self-organizing neural network, submitted, 2009. 8853, 8858

Thomson, R. E. and Fine, I. V.: Estimating Mixed Layer Depth from Oceanic Profile Data, J. Atmos. Ocean. Tech., 20, 319–329, 2002. 8856

Watson, A. J., Robinson, C., Robinson, J., Williams, P., and Fasham, M.: Spatial variability in the sink for atmospheric carbon dioxide in the North Atlantic, Nature, 350, 50–53, 1991. 8866

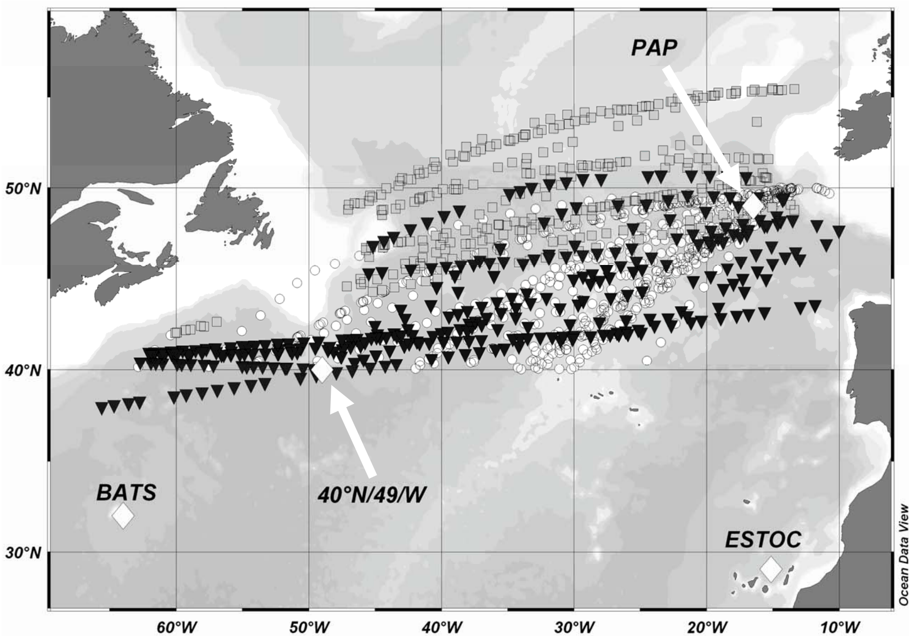

Fig. 1. Location of samples used in this study. Triangles denote samples taken in 2002 and 2003, squares denote samples taken since 2005. For validation purposes we also used data from another VOS line (UK-Caribbean), that was sampled in 2002/2003 by the National Oceanographic Center (NOC), Southampton (circles). The diamonds denote the position of the three time series staions BATS, ESTOC and PAP, as well as one location that is used for demonstration (refer to Fig. 6).

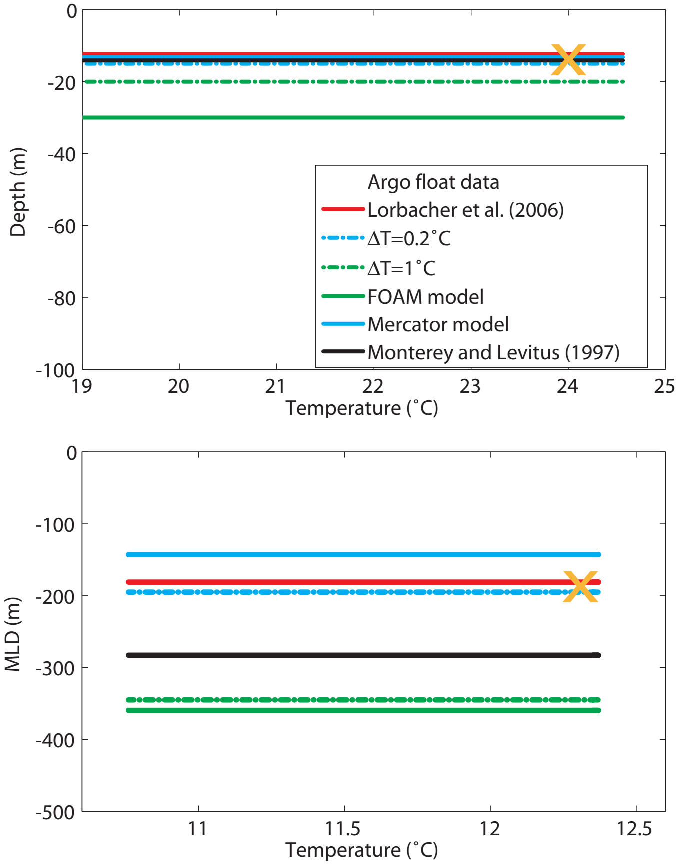

Fig. 2. Examples of two vertical temperature profiles from ARGO floats with the MLD assigned using various techniques or sources. The orange Xs denote the eyeball reference MLD. Top: Summer temperature profile. Bottom: Winter temperature profile.

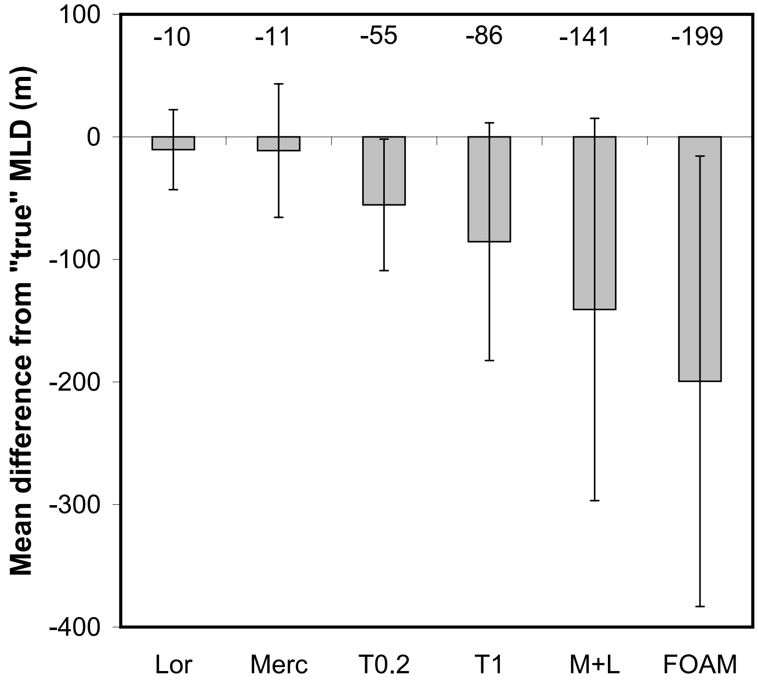

Fig. 3. Comparison of MLD estimates. The bars denote the mean difference between the eyeball defined MLD and the respective estimated MLD for 31 profiles. The exact mean differences are shown above each bar. Negative values indicate that the product defines a deeper MLD than the eyeball reference and vice versa. The error bars are the standard deviation (1σ). Abbrevations: Lor: criterion of Lorbacher et al. (2006), Merc: data from Mercator model, T0.2: temperature difference criterion with $\Delta T = 0.2^{\circ}$C, T1: temperature difference criterion with $\Delta T = 1^{\circ}$C, M+L: data from Monterey and Levitus (1997) climatology, FOAM: data from FOAM model.

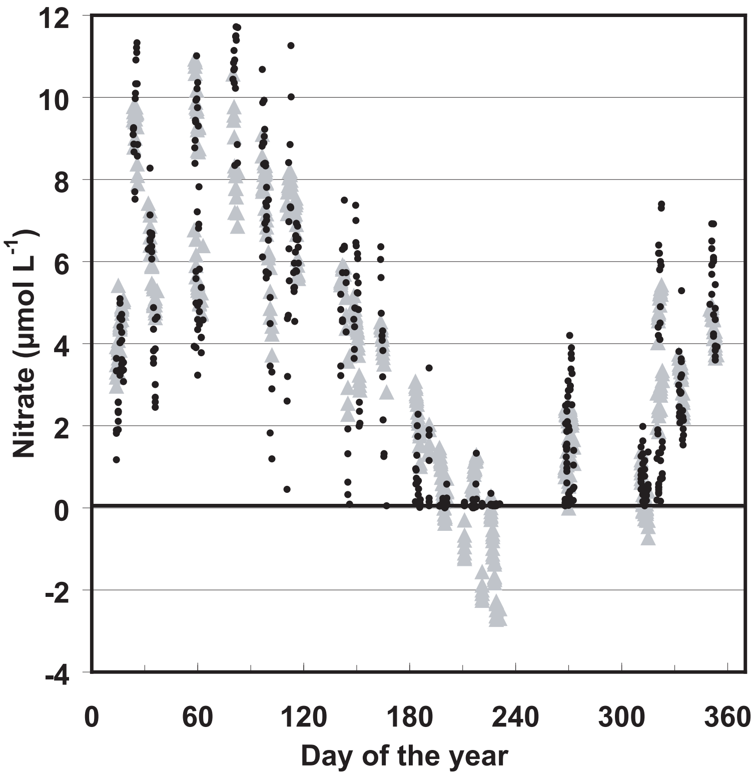

Fig. 4. Surface nitrate concentration versus day of the year for all data taken between 2002 and 2007. Black dots are the measured concentrations and grey triangles denote predicted concentrations.

BGD

6, 8851–8881, 2009

Title Page
Abstract
Introduction
Conclusions
References
Tables
Figures
◂
▸
◂
▸
Back
Close
Full Screen / Esc
Printer-friendly Version
Interactive Discussion

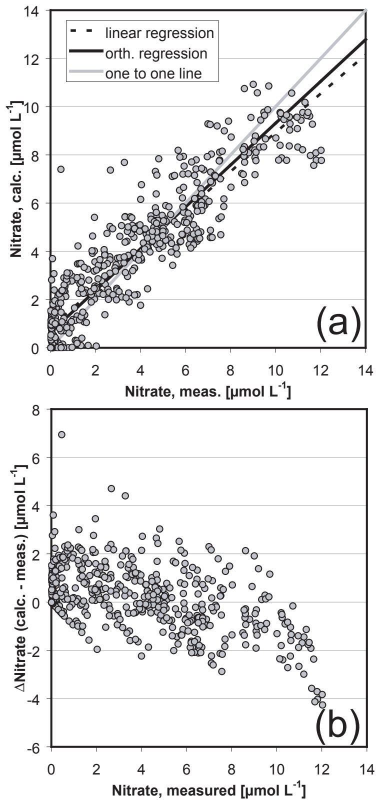

Fig. 5. (a): Calculated versus measured nitrate. The solid grey line represents the 1:1 relation, the dashed line the standard linear regression and the solid black line the orthogonal regression line. **(b)**: Difference of calculated and measured nitrate versus measured nitrate.

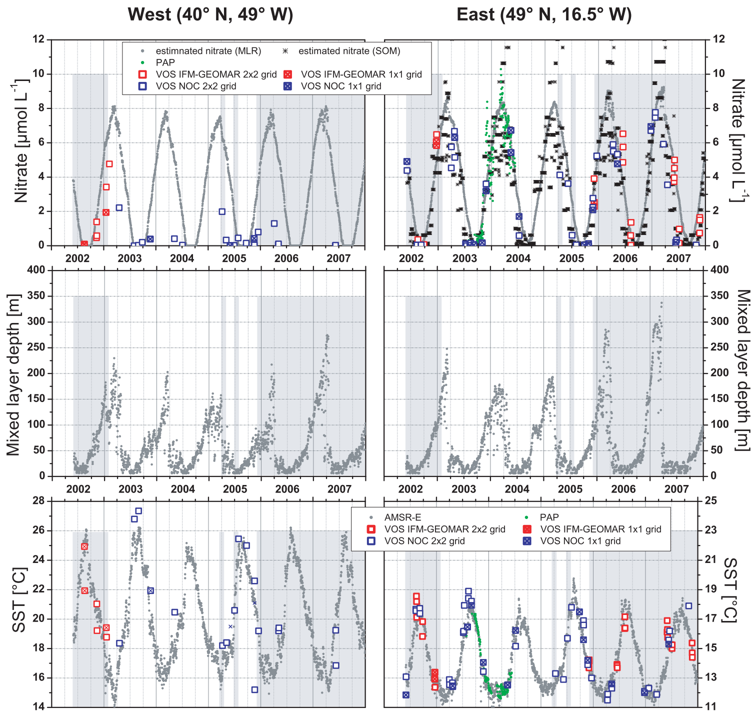

Fig. 6. Seasonality of nitrate, MLD and SST for the time period between 2002 and 2007 for a single location in the western and eastern part (PAP site) of the North Atlantic, respectively. The upper panels show the nitrate concentration calculated with the MLR and SOM, respectively. Nitrate measurements from PAP mooring and VOS lines that passed within a 1°×1° and 2°×2° grid cell, respectively, are shown. The middle panels show the MLD taken from Mercator (mean value of ±0.5° Lat/Lon around the location). The lower two panels show the SST from AMSR-E (mean value of ±0.5° Lat/Lon around the location) and measured SST from VOS lines. Also shown are the SST measurements from the PAP site in the eastern part.

BGD

6, 8851–8881, 2009

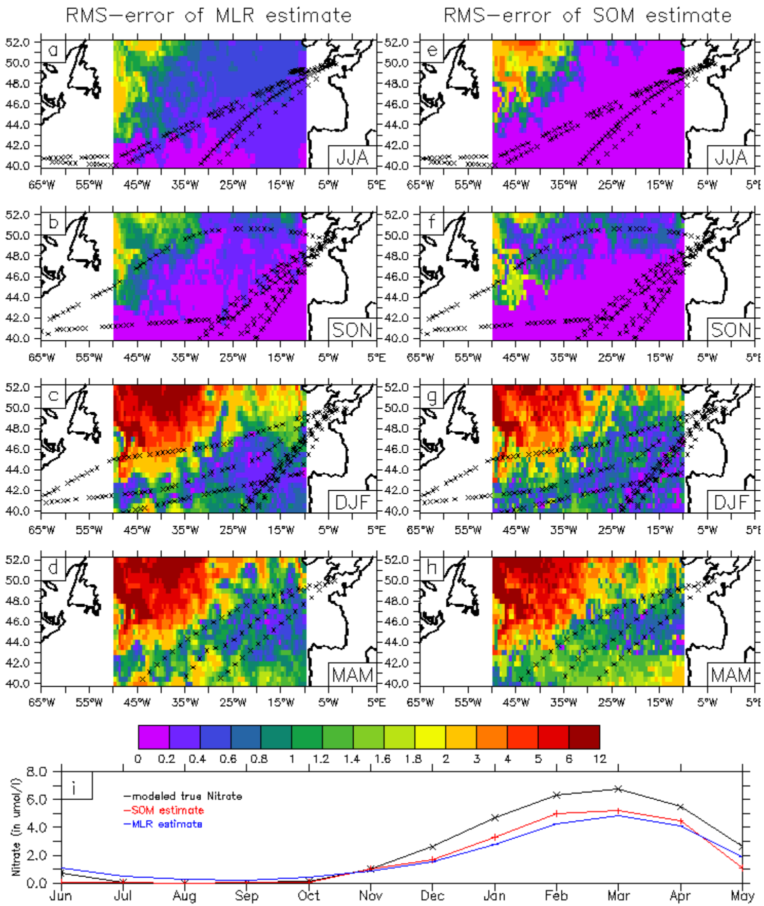

Fig. 7. RMS errors for nitrate estimates in μmol L^{-1} using a MLR **(a–d)** or SOM **(e–h)** technique in summer, fall, winter and spring, respectively. (i) Annual cycle of simulated "true" nitrate (black), and nitrate estimates using the SOM (red) or MLR (blue) technique for the region shown in (a–h). RMS errors and annual cyles were calculated using a biogeochmical model.

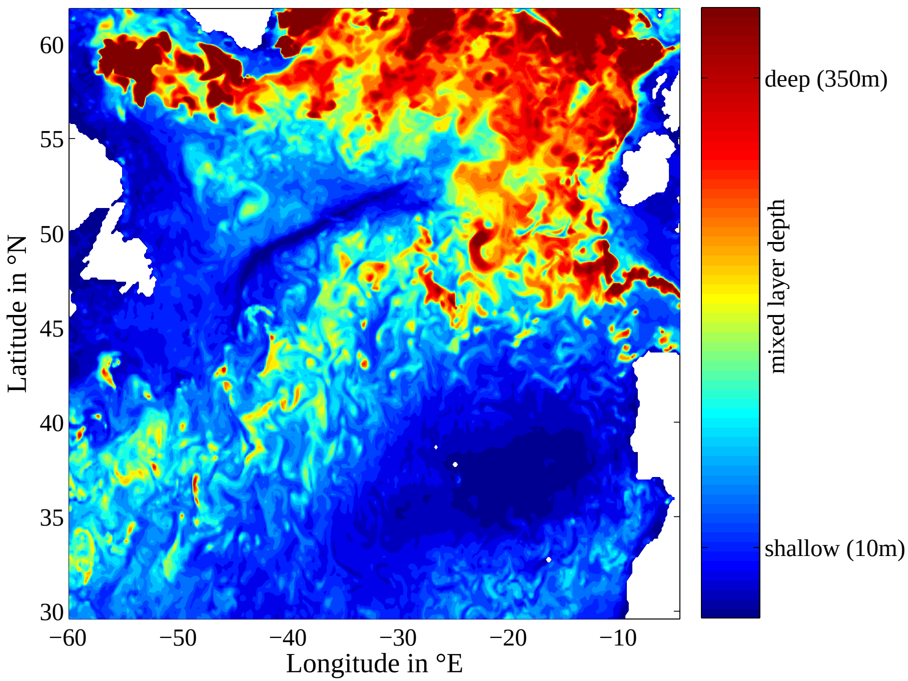

Fig. 8. MLD for 10 March, 2006 as calculated by Mercator.

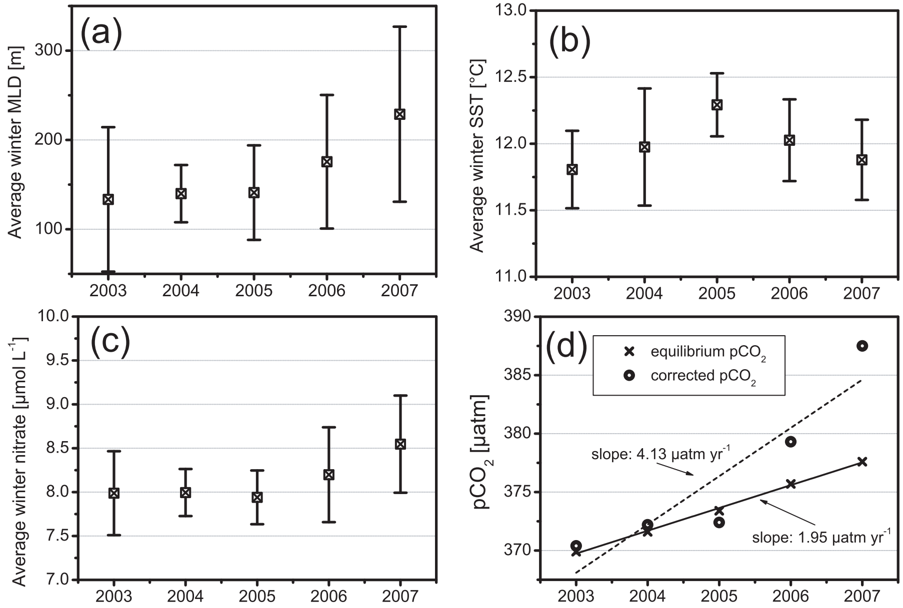

Fig. 9. (a–c) Average values of wintertime (February, March) MLD, SST and nitrate estimates from MLR at the location of PAP site. Error bars are standard deviations (1 σ). **(d)** Seawater $p\mathrm{CO_2}$ that is in equilibrium with the atmosphere and corrected for the extra amount of DIC associated with the extra nitrate.